Materials Science-Poland, 36(4), 2018, pp. 530-536
http://www.materialsscience.pwr.wroc.pl/
DOI: 10.2478/msp-2018-0080

Electrical and optical properties of new Pr^{3+}-doped $PbWO_4$ ceramics

TADEUSZ GROŃ[1,*], MAGDALENA PIĄTKOWSKA[2], ELŻBIETA TOMASZEWICZ[2], BOGDAN SAWICKI[1], PIOTR URBANOWICZ[1], HENRYK DUDA[1]

[1]University of Silesia, Institute of Physics, Uniwersytecka 4, 40-007 Katowice, Poland
[2]West Pomeranian University of Technology, Faculty of Chemical Technology and Engineering, Department of Inorganic and Analytical Chemistry, Al. Piastów 42, 71-065 Szczecin, Poland

Polycrystalline samples of new scheelite-type tungstates, $Pb_{1-3x}\square_xPr_{2x}WO_4$ with $0.0098 \leqslant x \leqslant 0.20$, where $\square$ denotes cationic vacancies have been successfully prepared by a high-temperature solid-state reaction method using $Pr_2(WO_4)_3$ and $PbWO_4$ as the starting reactants. The influence of the Pr^{3+} substitution in the scheelite framework on the structure and optical properties of prepared new ceramic materials has been examined using powder X-ray diffraction method (XRD) and UV-Vis-NIR spectroscopy. The results of dielectric studies of $Pb_{1-3x}\square_xPr_{2x}WO_4$ samples showed both low values of dielectric constant (below 14) and loss tangent (below 0.2). The electrical conductivity and thermoelectric power measurements revealed a low conductivity ($\sim 2 \times 10^{-9}$ S/m) and the sign change of thermoelectric power around the temperature of 366 K suggesting the p-n transition. These results are discussed in the context of vacancy, acceptor and donor levels as well as the Maxwell-Wagner model.

Keywords: *scheelite-type structure; optical properties; electrical conductivity; thermoelectric power*

1. Introduction

Lead tungstate ($PbWO_4$) is a popular scintillating material for use in the new generation of high-energy physics because of its relatively high density, fast scintillation decay constant, and resistance to radiation damage. These properties are particularly important for the new designed $PbWO_4$ instruments used in the Large Hadron Collider (at CERN) since the new accelerator generates high energy particles at high beam luminosity [1–15]. At room temperature, lead tungstate presents scheelite-type tetragonal structure, belonging to $I4_1/a$ space group [16, 17]. RE^{3+}-doped $PbWO_4$ exhibits good photoluminescence and it is a promising laser host [18–21]. Recently, the microcrystalline samples of new $Pb_{1-3x}\square_xPr_{2x}(MoO_4)_{1-3x}(WO_4)_{3x}$ solid solution, where x can reach the maximum value of 0.2222 and $\square$ means cationic vacancies, have been successfully synthesized by us [22]. Lead molybdate ($PbMoO_4$) and praseodymium tungstate ($Pr_2(WO_4)_3$) were used as the starting reactants for solid state synthesis [22]. The presence of cationic vacancies is due to the need of compensation of the excess positive charge resulting from the substitution of divalent Pb^{2+} ions by trivalent Pr^{3+} ones [22]. According to the X-ray diffraction analysis the $Pb_{1-3x}\square_xPr_{2x}(MoO_4)_{1-3x}(WO_4)_{3x}$ samples crystallize in the scheelite-type tetragonal symmetry, with $I4_1/a$ space group [22]. The introduction of cationic dopant (Pr^{3+}) to $PbMoO_4$ matrix significantly affects thermal and spectroscopic properties of the new ceramic materials. Both, $PbMoO_4$ and $Pb_{1-3x}\square_xPr_{2x}(MoO_4)_{1-3x}(WO_4)_{3x}$ samples are insulators and their indirect band gap, E_g, is higher than 3 eV [22]. The observed band gap of the new lead and praseodymium mixed molybdato-tungstates shows a nonlinear variation with a change of Pr^{3+} concentration in the scheelite framework [22].

In the present work, the results on new $Pb_{1-3x}\square_xPr_{2x}WO_4$ solid solution for $0.0098 \leqslant x \leqslant 0.20$ have been presented.

*E-mail: Tadeusz.Gron@us.edu.pl

Microcrystalline samples were prepared by the high-temperature annealing of $PbWO_4/Pr_2(WO_4)_3$ mixtures in air. The obtained new ceramics were characterized by XRD and UV-Vis-NIR techniques. Dielectric properties, electrical conductivity as well as thermoelectric power of $Pb_{1-3x}\square_xPr_{2x}WO_4$ samples were measured and discussed.

2. Experimental

The new microcrystalline lead and praseodymium tungstates $Pb_{1-3x}\square_xPr_{2x}WO_4$ have been successfully prepared by a high-temperature solid-state reaction of $PbWO_4$ with low-temperature polymorph of $Pr_2(WO_4)_3$ (monoclinic symmetry, space group C2/c [23]). The $PbWO_4/Pr_2(WO_4)_3$ mixtures with a different content of praseodymium tungstate, i.e. 1.00 mol%, 10.00 mol% and 33.33 mol% were heated in air, at temperatures from 1173 K to 1298 K in 12 h sintering stages. After each heating stage, the samples were cooled slowly down to ambient temperature, and ground in an agate mortar.

Powder XRD patterns were collected in the 10° to 100° 2θ range with the scanning step 0.013° on a EMPYREAN II diffractometer (PANanalytical) using $CuK\alpha_{1,2}$ radiation (λ = 0.15415 nm). They were analyzed by a High-Score Plus 4.0 software. First successive diffraction lines recorded within 2θ ($CuK\alpha$) 10° to 80° region were selected for indexing procedure and calculating the unit cell parameters performed by means of a POWDER software [24]. UV-Vis-NIR diffuse reflectance spectra were recorded at room temperature and in the wavelength range of 200 nm to 1000 nm using a JASCO-V670 spectrophotometer equipped with an integrating sphere. Broadband dielectric spectroscopy measurements were carried out using pellets, polished and sputtered with ~80 nm Ag electrodes in a frequency range of 5×10^2 Hz to 1×10^6 Hz using a Novocontrol Alpha impedance analyzer and in the temperature range of 76 K to 400 K. More details are available in the literature [25, 26]. The electrical conductivity (σT) of $Pb_{1-3x}\square_xPr_{2x}WO_4$ has been measured in the intrinsic region with the aid of DC method in the temperature range of 300 K to 400 K using a KEITHLEY 6517B electrometer/high resistance meter. The thermoelectric power S(T) was measured in the temperature range of 300 K to 600 K with the aid of a Seebeck effect measurement system (MMR Technologies, Inc., USA).

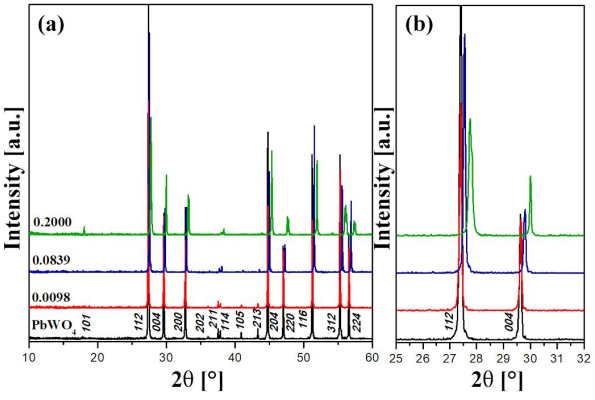

Fig. 1. (a) XRD patterns of $PbWO_4$ and $Pb_{1-3x}\square_xPr2xWO_4$ samples with $0.0098 \leqslant x \leqslant 0.20$ in the range of 2θ from 10° to 60°; (b) XRD patterns of the samples under study with the (1 1 2)/(0 0 4) diffraction peaks in the range of 2θ of 25° to 32°.

3. Results and discussion

The powder XRD patterns of lead tungstate and $Pb_{1-3x}\square_xPr_{2x}WO_4$ samples with different values of x parameter are shown in Fig. 1a. All observed diffraction lines are very sharp and strong, indicating good crystallinity of the as-prepared ceramic materials. Additionally, they are shifted towards higher 2θ angle with increasing praseodymium content (Fig. 1b). All the peaks of XRD patterns were successfully indexed with the scheelite-type structure belonging to the $I4_1/a$ space group. The calculated lattice parameters are: for $PbWO_4$: a = b = 5.46665 Å, c = 12.0567 Å; for $Pb_{1-3x}\square_xPr_{2x}WO_4$: a = b = 5.46436 Å, c = 12.0498 Å (for x = 0.0098); a = b = 5.43909 Å, c = 12.19916 Å (for x = 0.0839) and a = b = 5.38981 Å, c = 11.8864 Å (for x = 0.20). Both, the lattice constants and volume

calculated for the samples under study obey Vegard law, i.e. are nearly linear function of x parameter.

The band gap energy, E_g, is an important property of materials that determines their applications in optoelectronics. The band gap of bulk $PbWO_4$ and $Pb_{1-3x}\square_xPr_{2x}WO_4$ for various values of x parameter were determined from their UV-Vis-NIR diffuse reflectance spectra shown in Fig. 2a.

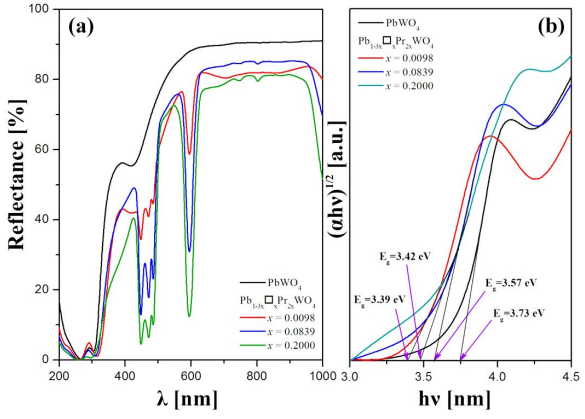

Fig. 2. (a) UV-Vis-NIR diffuse reflectance spectra of $PbWO_4$ and $Pb_{1-3x}\square_xPr_{2x}WO_4$ ceramics with various values of x parameter; (b) plots of $(\alpha h\nu)^{1/2}$ vs. hν and determined indirect band gap energy E_g.

The diffuse reflectance data were converted into absorption ones using the Kubelka-Munk function [27] defined as follows:

$$F(R) = (1-R)^2/2R \tag{1}$$

where R is a reflectance, F(R) is the Kubelka-Munk function. It is known that the optical band gap energy E_g is related with an absorption coefficient α and photon energy by the equation proposed by Wood and Tauc [28]:

$$\alpha h\nu = F(R)\cdot h\nu = A(h\nu E_g)^n \tag{2}$$

where A is a constant characteristic of the material under study, h is the Planck constant, ν is the light frequency. The n parameter is a constant which may take values 1/2, 2, 3/2 or 3 for allowed direct, allowed indirect, forbidden direct and forbidden indirect electronic transition, respectively. The plots of $(\alpha h\nu)^{1/2}$ versus hν derived from the reflectance data for pure matrix and $Pb_{1-3x}\square_xPr_{2x}WO_4$ samples are shown in Fig. 2b. The optical band gap of each sample was approximated by extrapolating the linear part of the plot of $(\alpha h\nu\square^{1/2}$ to zero (according to the procedure used by us in our previous papers [22, 25, 26]). The value of indirect band gap for $PbWO_4$ was found to be 3.73 eV (Fig. 2b). The observed indirect band gap for each Pr-doped sample is clearly smaller than E_g for the pure matrix and it was found to be 3.39 eV (x = 0.0098), 3.57 eV (x = 0.0839), and 3.42 eV (x = 0.20) (Fig. 2b). The nonlinear dependence of E_g on the value of x parameter has also been observed. The results of the band energy gap determination (Fig. 2b) and small values of the electrical conductivity $\sigma \sim 2\times10^{-9}$ S/m with their poor temperature dependence (Fig. 3) suggest the insulating properties of Pr-doped tungstates under study. The temperature dependence of thermopower, S(T), within the temperature range of 300 K to 600 K (Fig. 4) showed the p-n transition around the temperature of 366 K indicating mainly n-type residual conductivity, rarely p-type one, probably due to predominant contribution of oxygen than cationic vacancies. The sign change observed in S(T) dependence may be due to the existence of shallower vacancy acceptor levels, activated at lower temperatures, and deeper vacancy donor levels, activated at higher temperatures. Similar behavior we have observed in other RE molybdates and tungstates such as: $Cd_{1-3x}\square_xGd_{2x}MoO_4$ [25], $AgY_{1-x}(Gd,Nd)_x(WO_4)_2$ [25], $MRE_2W_2O_{10}$ (M = Cd, Co, Mn; RE = Y, Nd, Sm–Er) [25], and $RE_2W_2O_9$ (RE = Pr, Sm–Gd) [26]. It seems natural that when the energy gap is wider than 3.0 eV, the electrons cannot only be activated by thermal energy kT from the valence band to the conduction band.

Dielectric constant ε_r obtained for $Pb_{1-3x}\square_xPr_{2x}WO_4$ tungstates weakly depends on temperature and frequency (Fig. 5 to Fig. 7). It reaches low values, i.e. below 9, 14 and 10 for x = 0.0098, 0.0839 and 0.2000, respectively. The loss tangent, tanδ, shows a similar behavior and its value does not exceed 0.2 for x = 0.0098

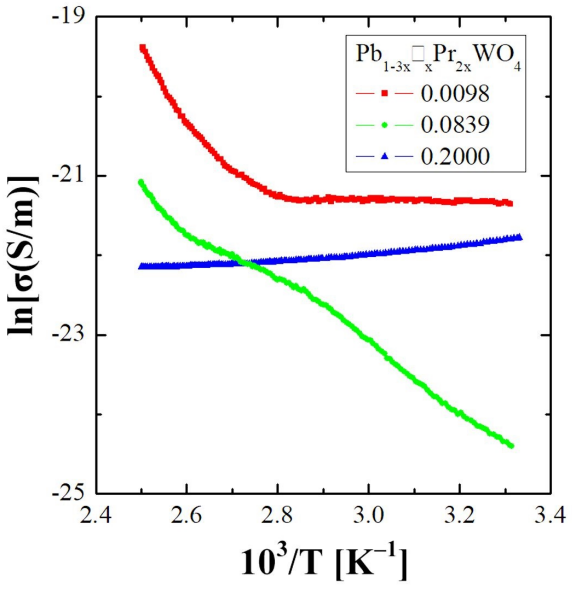

Fig. 3. Electrical conductivity lnσ vs. temperature 10^3/T for $Pb_{1-3x}\square_xPr_{2x}WO_4$.

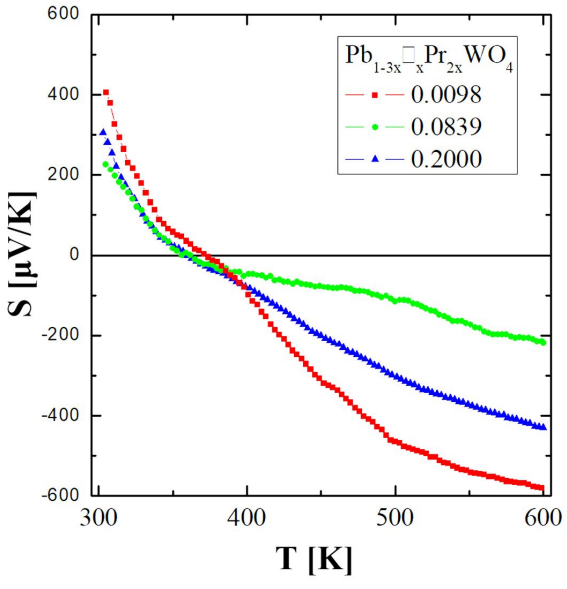

Fig. 4. Thermoelectric power S vs. temperature T for $Pb_{1-3x}\square_xPr_{2x}WO_4$.

(Fig. 8 to Fig. 10). For the remaining samples tanδ was found to be below 0.017 (Fig. 8 to Fig. 10). For this reason, tungstates under study are good dielectrics for the production of lossless capacitors. Generally, the low values of electrical conductivity, dielectric constant, and loss tangent observed for Pr-doped materials may suggest the presence of orientation polarization. It is also possible that the ceramics under study may create boundary phases and insulating areas "immersed" in almost not-conducting solid material which can be well described with the help of a double array model of a condenser called the Maxwell-Wagner model [29]. It can finally lead to the accumulation of induced charge or to blocking of the current cross-section by the boundary phases under the influence of the applied external electric field [30]. Most of the (charged) traps do reside in the grain boundaries with the depletion layers reaching into the adjacent grains.

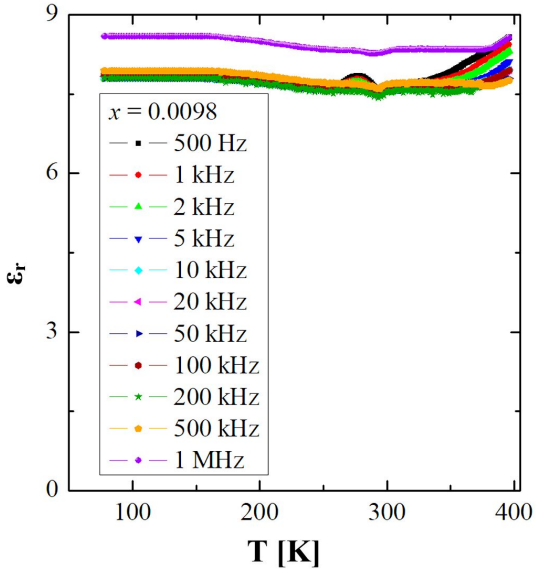

Fig. 5. Dielectric constant ε_r vs. temperature T for x = 0.0098 in the frequency range of 500 Hz to 1 MHz.

In dielectrics treated as a system of neutral atoms in which there are no free electrons, after ionization of an atom, the electron is moving freely in the surrounding medium consisting of polarizable atoms and in the field of remaining positive ions. Thus, the ionization energy must be decreased because this field is screened by the polarization of the surrounding atoms [31]. In the lanthanide elements and their compounds the unpaired 4f electrons are quite effectively screened from environmental effects by overlying s and p electrons [32]. In turn, in lead there are paired 5d electrons.

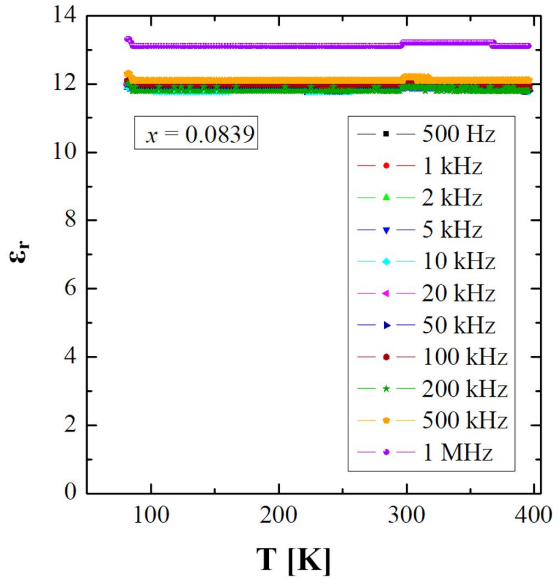

Fig. 6. Dielectric constant ε_r vs. temperature T for x = 0.0839 in the frequency range of 500 Hz to 1 MHz.

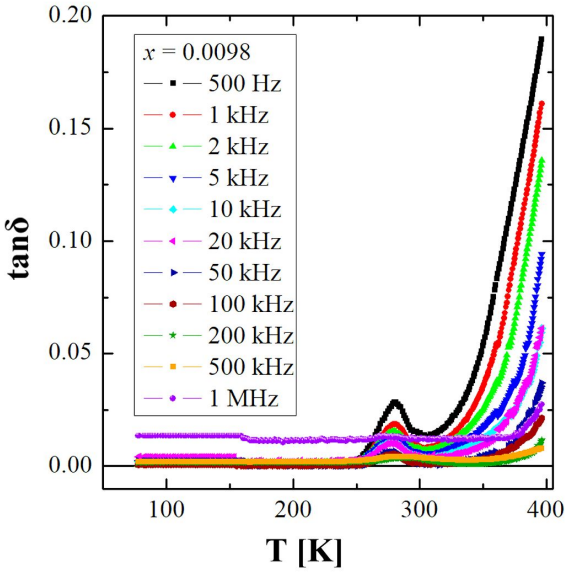

Fig. 8. Loss tangent tanδ vs. temperature T for x = 0.0098 in the frequency range of 500 Hz to 1 MHz.

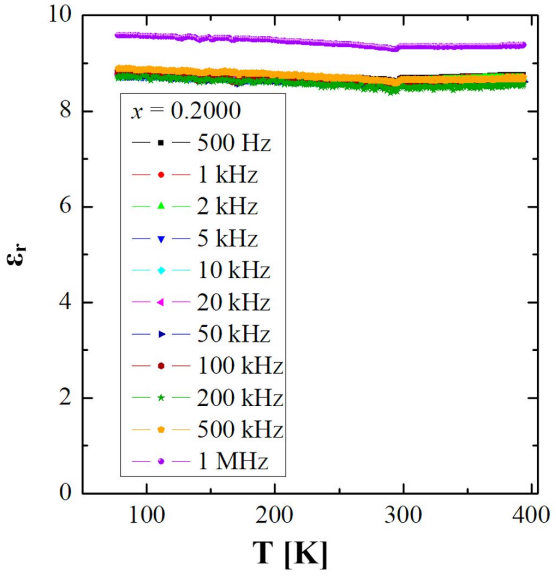

Fig. 7. Dielectric constant ε_r vs. temperature T for x = 0.2000 in the frequency range of 500 Hz to 1 MHz.

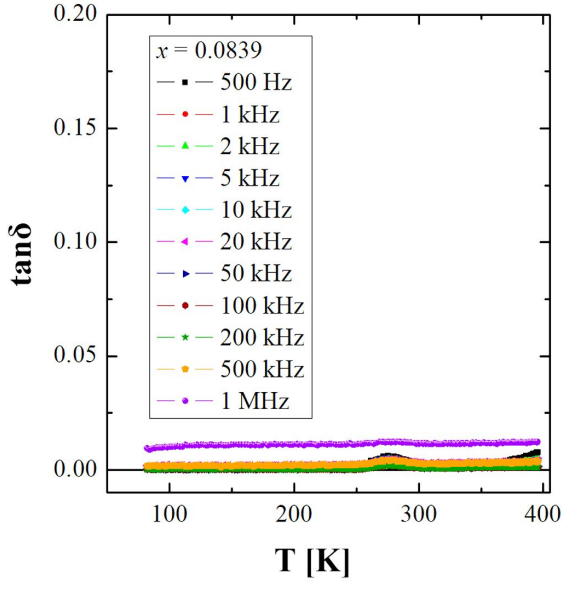

Fig. 9. Loss tangent tanδ vs. temperature T for x = 0.0839 in the frequency range of 500 Hz to 1 MHz.

4. Conclusions

Microcrystalline samples of $Pb_{1-3x}\square_xPr_{2x}WO_4$ solid solution with various values of x parameter have been prepared by a high-temperature sintering of $PbWO_4$ with $Pr_2(WO_4)_3$ used as the initial reactants and mixed in different molar ratios. It was found that all Pr-doped tungstates

have the scheelite-type structure, with the $I4_1/a$ space group. The indirect band gap E_g for pure matrix $PbWO_4$ and Pr-doped ceramics is higher than 3.0 eV. The nonlinear dependence of E_g on the value of x parameter was observed. All samples turned out to be insulators with small values of permittivity, loss tangent, and electrical conductivity. For this reason, both the pure matrix and the Pr-doped samples can be considered as good dielectrics useful for a production of lossless capacitors. The sign change of thermoelectric power during temperature increase may be due to the existence of vacancy acceptor and donor levels.

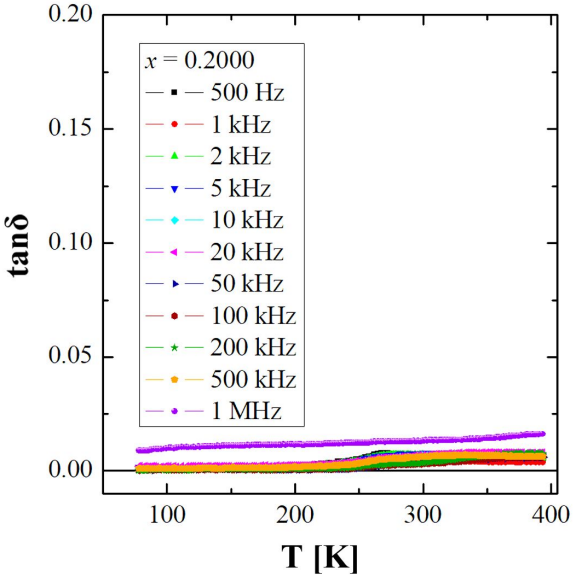

Fig. 10. Loss tangent tanδ vs. temperature T for x = 0.2000 in the frequency range of 500 Hz to 1 MHz.

Acknowledgements

The authors are also grateful to the workshop team of the Institute of Physics, University of Silesia, for providing practical and technical assistance in the measurements of broadband dielectric spectroscopy.

References

[1] NOVOTNY R., BECK R., DÖRING W., HEJNY V., HOFSTAETTER A., KORZHIK M., METAG V., RÖMER K., STRÖHER H., *Radiat. Meas.,* 33 (2001), 615.

[2] KOBAYASHI M., ISHII M., USUKI Y., *Nucl. Instr. Meth. Phys. Res. A,* 406 (1998), 442.

[3] FELLER R.P., GENDNER N., HOLM U., JOHNSON K.F., MEYER-LARSEN A., THIES S., *Nucl. Instr. Meth. Phys. Res. A,* 486 (2002), 785.

[4] LECOMTE P., LUCKEY D., NESSI-TEDALDI F., PAUSS F., RENKER D., *Nucl. Instr. Meth. Phys. Res. A,* 587 (2008), 266.

[5] HUHTINEN M., LECOMTE P., LUCKEY D., NESSI-TEDALDI F., PAUSS F., *Nucl. Instr. Meth. Phys. Res. A,* 545 (2005), 63.

[6] KOBAYASHI M., USUKI Y., ISHII M., YAZAWA T., HARA K., TANAKA M., NIKL M., BACCARO S., CECILIA A., DIEMOZ M., DAFINEI I., *Nucl. Instr. Meth. Phys. Res. A,* 404 (1998), 149.

[7] LECOQ P., DAFINEI I., AUFFRAY E., SCHNEEGANS M., KORZHIK M.V., MISSEVITCH O.V., PAVLENKO V.B., FEDOROV A.A., ANNENKOV A.N., KOSTYLEV V.L., LIGUN V.D., *Nucl. Instr. Meth. Phys. Res. A,* 365 (1995), 291.

[8] BACCARO S., BORGIA B., CECILIA A., DAFINEI I., DIEMOZ M., NIKL M., MONTECCHI M., *Radiat. Phys. Chem.,* 52 (1998), 635.

[9] BURACHAS S., BODNAR V., BORODENKO YU., KATRUNOV K., MARTINOV V., NAGORNAYA L., RYZHIKOV V., TAMULAITIS G., GUTBROD H., MANKO V., *J. Cryst. Growth*, 198/199 (1999), 881.

[10] NESSI-TEDALDI F., *Nucl. Instr. Meth. Phys. Res. A,* 408 (1998), 266.

[11] LONGO E., *Nucl. Instr. Meth. Phys. Res. A,* 384 (1996), 225.

[12] ORGANTINI G., *Nucl. Phys. B,* 61B (1998), 59.

[13] SHIMIZU H., SAKAMOTO Y., HASHIMOTO T., ABE K., ASANO Y., KINASHI T., MATSUMOTO T., MATSUMURA T., OKUNO H., YOSHIDA H.Y., *Nucl. Instr. Meth. Phys. Res. A,* 447 (200), 467.

[14] CAVALLARI F., *Nucl. Phys. B*, 61B (1998), 449.

[15] KOZMA P., BAJGAR R., KOZMA P. JR., *Rad. Phys. Chem.*, 65 (2002), 127.

[16] GONG G., SHEN D., REN G., ZHANG H., YIN Z., *J. Cryst. Growth,* 235 (2002), 320.

[17] MOREAU J.M., GLADYSHEVSKII R.E., GALEZ P.H., PEIGNEUX J.P., KORZHIK M.V., *J. Alloy. Compd.,* 284 (1999), 104.

[18] HUANG Y., FENG X., XU Z., ZHAO G., HUANG G., LI S., *Solid State Commun.,* 127 (2003), 1.

[19] CHEN W., INAGAWA Y., OMATSU T., TATEDA M., TAKEUCHI N., USUKI Y., *Opt. Commun.,* 194 (2001), 401.

[20] HUANG Y., SEO H.J., FENG Q., YUAN S., *Mater. Sci. Eng. B-Adv*, 121 (2005), 103.

[21] HUANG Y., ZHU W., FENG X., LIU Z., MAN Z., YIN Z., *Opt. Mat.,* 23 (2003), 443.

[22] PIĄTKOWSKA M., TOMASZEWICZ E., *J. Therm. Anal. Calorim.*, 126 (2016), 111.

[23] NASSAU K., LEVINSTEIN H.J., LOIACONO G.M., *J. Phys. Chem. Solids,* 26 (1965), 1805.

[24] TAUPIN D., *J. Appl. Crystallogr.,* 6 (1973), 380.

[25] SAWICKI B., GROŃ T., TOMASZEWICZ E., DUDA H., GÓRNY K., *Ceram. Int.,* 41 (2015), 13080.
[26] URBANOWICZ P., PIĄTKOWSKA M., SAWICKI B., GROŃ T., KUKUŁA Z., TOMASZEWICZ E., *J. Eur. Ceram. Soc.,* 35 (2015), 4189.
[27] TAUC J., GRIGOROVICI R., VANCU A., *Phys. Status Solidi*, 15 (1966), 627.
[28] WOOD D.L., TAUC J., *Phys. Rev. B.,* 5 (1972), 3144.
[29] HIPPEL VON A., *Dielectrics and Waves*, Artech House, London, 1995, p.228.
[30] KUANG W., NELSON S.O., *Trans. ASAE,* 41 (1998), 173.
[31] FRENKEL J., *Phys. Rev.,* 54 (1938) 647.
[32] EARNSHAW A., *Introduction to Magnetochemistry*, Academic Press, London and New York, 1968, p.29.

Received 2016-06-13
Accepted 2018-07-26